LANGMUIR

Article

pubs.acs.org/Langmuir

Tailoring the Electrochemical Properties of Carbon Nanotube Modified Indium Tin Oxide via *in Situ* Grafting of Aryl Diazonium

Jacqueline M. Hicks,[†] Zhi Yi Wong,[†] David J. Scurr,[†] Nigel Silman,[‡] Simon K. Jackson,[§] Paula M. Mendes,[∥] Jonathan W. Aylott,[†] and Frankie J. Rawson*[,†]

[†]School of Pharmacy, University of Nottingham, Nottingham NG7 2RD, U.K.

[‡]Public Health England, Porton Down, Salisbury SP4 OJG, U.K.

[§]School of Biomedical & Healthcare Sciences, University of Plymouth, Drake Circus, Plymouth PL4 8AA, U.K.

[∥]School of Chemical Engineering, University of Birmingham, Birmingham B15 2TT, U.K.

Supporting Information

ABSTRACT: Our ability to tailor the electronic properties of surfaces by nanomodification is paramount for various applications, including development of sensing, fuel cell, and solar technologies. Moreover, in order to improve the rational design of conducting surfaces, an improved understanding of structure/function relationships of nanomodifications and effect they have on the underlying electronic properties is required. Herein, we report on the tuning and optimization of the electrochemical properties of indium tin oxide (ITO) functionalized with single-walled carbon nanotubes (SWCNTs). This was achieved by controlling *in situ* grafting of aryl amine diazonium films on the nanoscale which were used to covalently tether SWCNTs. The structure/function relationship of these nanomodifications on the electronic properties of ITO was elucidated via time-of-flight secondary ion mass spectrometry and electrochemical and physical characterization techniques which has led to new mechanistic insights into the *in situ* grafting of diazonium. We discovered that the connecting bond is a nitro group which is covalently linked to a carbon on the aryl amine. The increased understanding of the surface chemistry gained through these studies enabled us to fabricate surfaces with optimized electron transfer kinetics. The knowledge gained from these studies allows for the rational design and tuning of the electronic properties of ITO-based conducting surfaces important for development of various electronic applications.

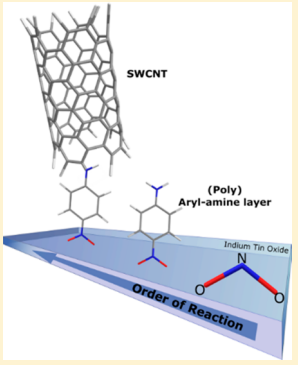

INTRODUCTION

There is a pressing requirement to tune the electronic properties of materials in order to advance the development of sensors, fuel cells, energy capture, and solar technologies. A more detailed knowledge of the structure/function relationship is required of the nanomodification techniques used for developing electronics. This will facilitate the rational design of conductive surfaces and optimize the development of technology. For example, particular attention has been paid in the use of carbon nanotubes (CNTs) as cellular sensing devices due to their ability to sense a wide range of moieties as well as their ability to penetrate into cells for intracellular measurements.[1−3] Our group have recently developed conducting electrodes that used indium tin oxide (ITO) modified with an aryl amine film via the *in situ* electrochemical grafting of aryl diazonium, which acted as an anchor layer, to which CNTs where attached for sensing cellular events[2−4] and mediating charge transfer from bacteria.[1]

Changes in cellular analytes that can be potentially detected by electrochemical sensing technology tend be at very low concentrations. Additionally, in applications where there is a requirement to facilitate charge transfer, such as in fuel cells, electrodes require optimization in order to maximize current, output, and efficiency.[4] Therefore, investigations are required to optimize the ITO platform to enhance sensing sensitivities and facilitate charge transfer. Importantly, no thorough studies have been performed to improve the electronic properties of ITO conducting surfaces using diazonium chemistry or details elucidated of the physicochemical structure/function relationships.

Diazonium chemistry has been attracting growing interest particularly in its ability to form organic layers that can covalently bind onto a variety of surfaces.[5] A majority of studies using diazonium chemistry to modify surfaces have focused on modification of gold and carbon surfaces[6−9] (see Table 1). Adaptation of indium tin oxide (ITO) surfaces with films via grafting of diazonium molecules has only recently been reported.[2,10,11] However, the underlying mechanism of diazonium attachment to an ITO substrate has largely gone unstudied until the work reported herein. The application of diazonium species are broad but have been important for functionalization of surfaces by immobilizing carbon nanotubes (CNTs)[2] and anchoring polymers[12] and applied to improving the electronic performance of microbial fuel cells.[13]

Received: February 13, 2017
Revised: April 21, 2017
Published: May 1, 2017

DOI: 10.1021/acs.langmuir.7b00494
Langmuir 2017, 33, 4924−4933

Table 1. Reaction Schemes of Diazonium Formation and Its Attachment to Surfaces As Reported[a]

Scheme	Substrate (s):	Schematic:	Refs:
1	n/a	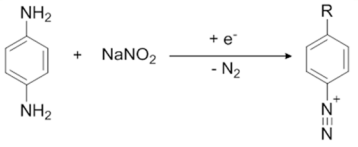	7
2	Carbon, Gold, Iron,	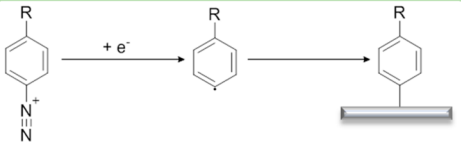	5, 6, 19, 31, 32, 32
3	Carbon, Gold, ITO,	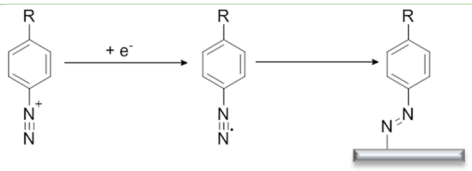	11, 18, 19, 31
4	Copper,	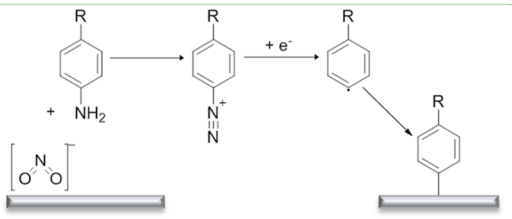	33
5		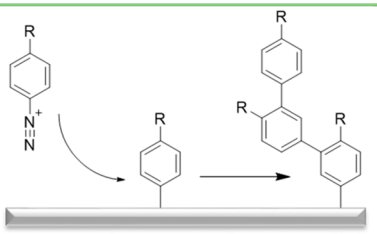	34, 35, 36

[a]Scheme 5 displays generic multilayer formation as described in the literature.

The grafting mechanisms that have been previously suggested at varying surfaces including gold, carbon, and ITO involve the formation of either a radical intermediate or a diazonium cation that reacts with the substrate (see Table 1). The assertion of the presence of a covalent bond between the surface and the diazonium ion is largely reliant on its stability and ability to withstand ultrasonic cleaning in a variety of solvents including hydrochloric acid and ammonium hydroxide.[6,14−16] The layer formed from the diazonium onto the varied material surfaces has also been shown to withstand extreme potentials in cyclic voltammetry experiments, giving further evidence of a strong covalent attachment.[17] The identity of this bond and the mechanism of binding are of great interest, though the general consensus is that either an aryl radical or a cation is formed from the diazonium, which then attaches to the surface. This mechanism of binding has been thought to produce a carbon-based bond directly from the benzene group to the surface independent of the surface chemistry.[5,6] There is, however, recent evidence of a mixed mechanism involving an azo phenyl group which can bind directly to the surface via its nitrogen atom.[18] More recently, an azo phenyl radical was shown to have been involved in the grafting of diazonium salts on metallic surface material.[19] There have also been literature reports that contradict the theory of electrochemically induced grafting of diazonium as the sole method of attachment, with evidence indicating that diazonium ions can graft to the surface spontaneously[19−21] as well as electrochemically.

The functionalization of conducting surfaces with carbon nanotubes (CNTs) to build electrochemical sensors has commonly been achieved through chemically coupling to surfaces modified with a molecular anchor. These molecular anchors include self-assembled monolayers (SAMs) or diazonium generated films which may contain functional groups such as carboxylic acid, amine, or hydroxyl groups. These functional groups are then used to couple CNTs to the surface. While SAMs form monolayers more consistently than diazonium-derived films, diazonium films have been shown to be more stable.[4,22−24]

CNTs display interesting electrochemical properties which are dependent on the length[25] of the nanotubes as well as the surface to which they are attached. CNTs have been studied on numerous surfaces such as glass,[26,27] metal-coated silicon wafers,[28] gold-coated SiO_2,[29] pyrolyzed photoresist electrodes,[4] and ITO.[2] Different methods exist for the attachment of CNTs to surfaces with the most common being chemical vapor deposition where the nanotubes are "grown" directly onto the

DOI: 10.1021/acs.langmuir.7b00494
Langmuir 2017, 33, 4924−4933

surface. Alternatively, CNTs can be covalently bound to surfaces either directly (dependent on the surface) or via a tether molecules. One example of which is a diazonium,[2,30] based electrochemical grafted aryl amine layer, which was then used to covalently tether carboxylated CNTs.

With the diverse uses and clear adaptability of diazonium-based organic films on surfaces, it is important to fully understand the mechanism behind their attachment to the surface. Therefore, the aim of the present work was to provide more detailed knowledge of the structure/function relationship of ITO surfaces modified with nanoscale films and the effect on their electronic properties. This allowed us to optimize the electron transfer kinetics of the electrode once the ITO-aryl films were functionalized with CNTs and gain insight into how the underlying film structure affects the end-sensor properties. We propose a new mechanism that for the formation of aryl amine film on ITO via the *in situ* electrochemical grafting of aryl diazonium. The knowledge gained from these studies allows for the rational design and tuning of electronic properties of ITO based conducting surfaces important for development of various electronic applications.

EXPERIMENTAL SECTION

Electrochemical Grafting of Surfaces. Corning low alkaline earth boroaluminosilicate glass, deposited with indium tin oxide (ITO) on one side, was purchased from Delta Technologies Limited and rinsed with HPLC grade ethanol and then distilled water before being exposed to UV light for an hour in a UV drawer (Bioforce Nanosciences). The ITO was then sonicated (Fisherbrand FB11021) in acetone twice each for 2 min and propan-2-ol for 30 s. In order to graft the aryl layer to the ITO, a 10 mM solution of *p*-phenylenediamine in 0.5 M hydrochloric acid was added to a 1 mol equiv of sodium nitrite in distilled water and allowed to react for 2 min to form 4-aminobenzenediazonium. The reaction solution was then added to the electrochemical cell with the ITO in place. The diazonium radical from the reaction mixture was electrochemically grafted to the ITO by chronoamperometry at a fixed potential at −0.6 V for 2 min (unless otherwise stated). The electrochemical surface area was defined by a silicon "O" ring and was approximately 7 mm in diameter.

Preparation of Carbon Nanotubes and Surface Attachment. Single-walled carbon nanotubes (SWCNTs) were obtained from Nanolab Inc. and were subsequently cut via acid treatment in concentrated sulfuric and nitric acid (3:1 mix) and sonicated for 10 h. The SWCNTs were then submerged into 1 L of distilled water overnight. The cut SWCNTs were then rinsed until a neutral pH was detected by vacuum filtration through a 0.22 μM hydrophilic PVDF filter (Millipore) and washed with Milli-Q water until the rinse water was close to neutral pH. The SWCNT containing filter was then dried in an oven overnight at 65 °C. In order to couple the SWCNTs to the aryl amine films on the ITO chip, suspensions of SWCNTs were prepared in DMSO. ITO−aryl surfaces were submerged in the CNT/DMSO suspension at a concentration of 0.2 mg mL^{-1}, containing 0.5 mg mL^{-1} dicyclohexylcarbodiimide (DCC). The reaction mixture was sonicated for 15 min and then placed in the oven at 60 °C for 18 h. Samples were then sonicated in acetone for 2 min and isopropyl alcohol for 10 s before being rinsed with Milli-Q water and dried with argon.

Time-of-Flight Secondary Ion Mass Spectroscopy (ToF-SIMS). ToF-SIMS was carried out using a ToF-SIMS IV (IONTOF GmbH) instrument in static mode. Static conditions were ensured by maintaining a primary ion dose density $<1 \times 10^{12}$ ions per cm^{-2}. A Bi_3^+ pulsed ion beam was used with a target current of ∼0.3 pA. Scans were taken (5 × 5 mm areas at a resolution of 100 pixels per mm) covering both a region with diazonium grafting (within the O ring) and a region where grafting did not occur (outside the O ring) as an internal control. Positive and negative data were collected and normalized to total ion peak intensity for comparison. ToF-SIMS data acquisition and analysis was performed using SurfaceLab 6 software (IONTOF GmbH). Further analysis including statistical tests were conducted with Graphpad Prism software. Samples analyzed are described by the length of time a potential is applied during electrografting with an additional control performed in which no electrochemical grafting was performed, which we term 0 s as no application of potential was applied but the sample was exposed to a solution of the *in situ* generated 4-aminobenzenediazonium.

Ellipsometry. The thickness of the aryl films on ITO were measured with a J.A. Woollam Co., Inc., spectroscopic ellipsometer α-SE and modeled with CompleteEASE software. Thicknesses were calculated in fast mode with the refractive index, n, and dispersion coefficient, k, calculated to be approximately 1.705 and 0.045, respectively, for the ITO layer and 1.713 and 0.011, respectively, when measuring the aryl layer as calculated by the CompleteEASE software. The ellipsometry model was based on multiple layers. The base of the surface being 1 mm of glass was inputted as a 7059 Cauchy substrate. Layer 1 was "ITO parametrized" (built into the software) to measure the thickness of the ITO; this was done for each individual sample for the ITO outside the grafted region in order to get a more accurate measurement of the aryl amine layer. Layer 3—to measure the thickness of the aryl amine—was a standard Cauchy layer with substrate backside correction on and back reflections set to 5% to take into account the near-transparent nature of our surfaces.

Atomic Force Microscopy (AFM). Depth analysis of samples was conducted by AFM depth profiling with an atomic force microscope (Dimension 3000, Veeco) with a NanoScope version:IIIa controller and NanoScope V531r1 software. All AFM images were obtained with a RTESPA-150 cantilever (BRUKER) with a resonant frequency of 150 kHz and a spring constant of 6 N m^{-1}. The samples were held on a metal stage and initially scanned in tapping mode with a scan size of 15 μm × 15 μm, a scan angle of 90°, and scan rate of 1 Hz to gain an initial idea of topography of the surface. The surface of the samples was then scratched in contact mode with a deflection set point of 8 V, scan size of 5 μm × 5 μm, scan angle of 0°, scan rate of 0.5 Hz, integral gain of 0.2, and a resolution of 512 × 512 pixels. Following this the tip was disengaged, and the sample was scanned for a second time in tapping mode again at 15 μm × 15 μm with the same settings as previously described.

Processing and analysis of the AFM images was performed with NanoScope Analysis 1.5. Images were "flattened" with the scratch area excluded in this function. The thickness of the aryl film was subsequently determined by the "step" function, which measured the difference in height between the scratched and unscratched regions.

XPS. XPS data were collected with a Kratos Axis Nova spectrometer. The X-ray source was monochromatic Al Kα with a working energy of 1486.6 eV. Spectra were collected with a 0° emission angle with a field of view of 700 μm × 300 μm. A pass energy of 160 eV was used for the survey scans and 20 eV for the high-resolution regions (C 1s, O 1s, and N 1s). CASA XPS curve-fitting software was used to analyze the spectra. Bare ITO, "0" s grafted, and "1" s grafted were analyzed with three repeats of each and three regions within each. Samples were analyzed at the National XPS EPRSC users service (NEXUS) at Newcastle University.

Stability Study. Samples were electrografted by applying a fixed potential of −0.6 V for either 1, 2, 4, 6, 8, or 10 s. These were then tested via cyclic voltammetry using a VersaStudio potentiostat cycling between 0.8 and −0.4 V at a scan rate of 100 mV/s. Samples were tested on the same day as grafting (day 0) and days 3, 5, and 7 postgrafting. Phosphate buffered saline (PBS) was used as a control solution while potassium ferricyannide (250 μM, in PBS) was utilized as a standard redox molecule. Bare, cleaned ITO was also tested on "day 0" as a control.

Scan Rate Study. Cyclic voltammetry studies were performed with an electrochemical cell with a surface area of 7.07 mm^2 (diameter 3 mm). Scan range was between 0.8 and −0.4 V starting at 0.8 V and switching at −0.4 V. For determination of the heterogeneous rate, constant scan rates were varied between 5 mV/s and 5 V/s. Potassium ferricyannide (250 μM) in phosphate buffered saline (PBS) was used

DOI: 10.1021/acs.langmuir.7b00494
Langmuir 2017, 33, 4924−4933

as an analyte and was purged of air with argon. Control scans were conducted with PBS at the two extreme scan rates. Ohmic drop was not compensated for at any scan rate.

Materials. All materials unless otherwise stated were obtained from Sigma-Aldrich.

RESULTS AND DISCUSSION

Characterization of the Aryl Amine Film. Our group[2] and others[10] have recently developed sensors that used ITO modified with an aryl amine film which acted as an anchor layer. We used this to functionalize surfaces with SWCNTs. The choice of the aryl diazonium is based on previous work done by the Rawson group. The amine terminal group is ideal for conjugating to the CNTs which have exposed carboxylic acid groups.[2,3]The SWCNT modified ITO was subsequently modified with an electrocatalyst.[3] Importantly, the electronic properties of the sensor-cell constructs were not optimized and constructed with an aryl film that was electrografted by applying a fixed potential of −0.6 V for 120 s.[2,4] This results in comparatively thick films—close to the maxima reported in the literature.[12,37] Initial investigations to establish the electrochemical nature of this relatively thick aryl amine film were therefore conducted. This was achieved by performing cyclic voltammetric experiments (Figure 1) on solutions of *in situ* generated aryl diazonium, thereby modifying the ITO with an aryl amine layer. Figure 1 demonstrates that the resulting film passivates the conductive nature of the ITO. The initial cyclic voltammogram (CV) obtained (Figure 1; CV1) with the in situ generated diazonium solution resulted in observing a reductive peak at −0.141 V, which after applying a fixed potential of −0.6 V for 120 s disappears (Figure 1; CV2). This has previously been seen on both ITO and gold.[18] This is presumed to be because a thick multilayered film has been formed[37] which increases the resistance of the film to the point that little to no current reaches the surface and therefore no additional aryl diazonium in solution can be reduced. In order to investigate the effect of film thickness on the final nanotube sensor construct, a physical and electrochemical characterization of the aryl film electrografted for different lengths of time was conducted before testing the films with the nanotubes.

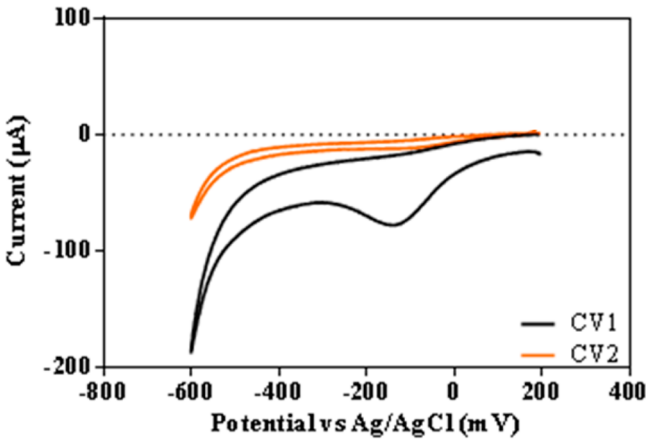

Figure 1. Typical cyclic voltammograms (CVs) obtained for solutions containing *p*-phenylenediamine and sodium nitrite at an ITO electrode before grafting (CV1) and after grafting with the aryl radical produced after 120 s (CV2) using fixed potential amperometry. CVs were conducted using an initial potential of 0.2 V and a vertex of −0.6 V at a scan rate of 0.1 V/s.

In order to determine the precise nature of the aryl amine film produced, time-of-flight secondary ion mass spectrometry (ToF-SIMS) was utilized to investigate how the surface chemistry changes with grafting time. Initial ToF-SIMS analysis of the ITO was conducted on samples electrochemically grafted for between 1 and 120 s, either scanned immediately after grafting (Day "0") or after 3 or 7 days, respectively. This allowed an assessment of the changes on the surface of the sample in order to examine the stability of the grafted surfaces as well as the effect of grafting time. If the CNT sensors were to ever be constructed on a large scale as a diagnostic device, for example, the stability of each step of their construction becomes important and could indeed become a limiting factor in their fabrication. Figures 2A and 2B show secondary ion images for indium (m/z = 114.91), including both grafted and nongrafted regions of the sample, for 4 and 120 s grafting time, respectively. These ion images highlight the differences in ion intensities within the grafted regions while also functioning as an internal control in areas which were not grafted. The grafting area was defined by use of an O-ring as detailed in the methods section.

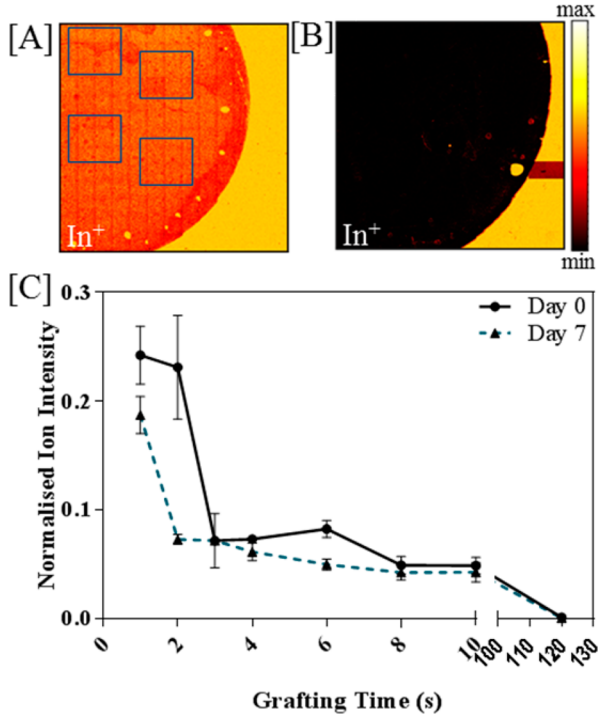

Figure 2. Secondary ion images for In^+ for [A] 4 s grafting and [B] 120 s grafting. The regions outlined in [A] represent the four regions of interest (ROI's) isolated in each sample within the reaction area to generate the mean ion intensities that are represented in [C] indium ion (m/z = 114.91) intensities for samples grafted between 1 and 120 s, scanned either on day of grafting (day 0) or day 7 postgrafting (±SD).

Figure 2C demonstrates that there is a decrease in indium ion intensity (within the grafted region) with increasing grafting time correlating to the increasing thickness of the bound aryl layer on the surface. The 120 s sample showed no detectable In^+ ions within the grafted region presumably due to the depth limits of the ion beam and the thickness of the layer. This is contrasted by the 4 s grafted sample as displayed in Figure 2A which shows some In^+ fragments but is still not as intense as

DOI: 10.1021/acs.langmuir.7b00494
Langmuir 2017, 33, 4924−4933

Table 2. Ellipsometry and AFM Depth Profiling Data of Samples Grafted for between 1 and 120 s (Values Displayed Are Mean Thickness in nm ± Standard Deviation)

grafting time (s)	1	2	4	6	8	10	120
ellipsometry	2.3 ± 0.3	2.3 ± 0.5	2.6 ± 0.4	2.6 ± 0.5	4.5 ± 2.9	4.6 ± 2.5	15.5 ± 2.4
AFM	2.9 ± 1.1	3.1 + 2.0	3.5 ± 1.6	4.7 ± 2.3	5.2 ± 1.9	5.4 ± 2.8	26.4 ± 4.2

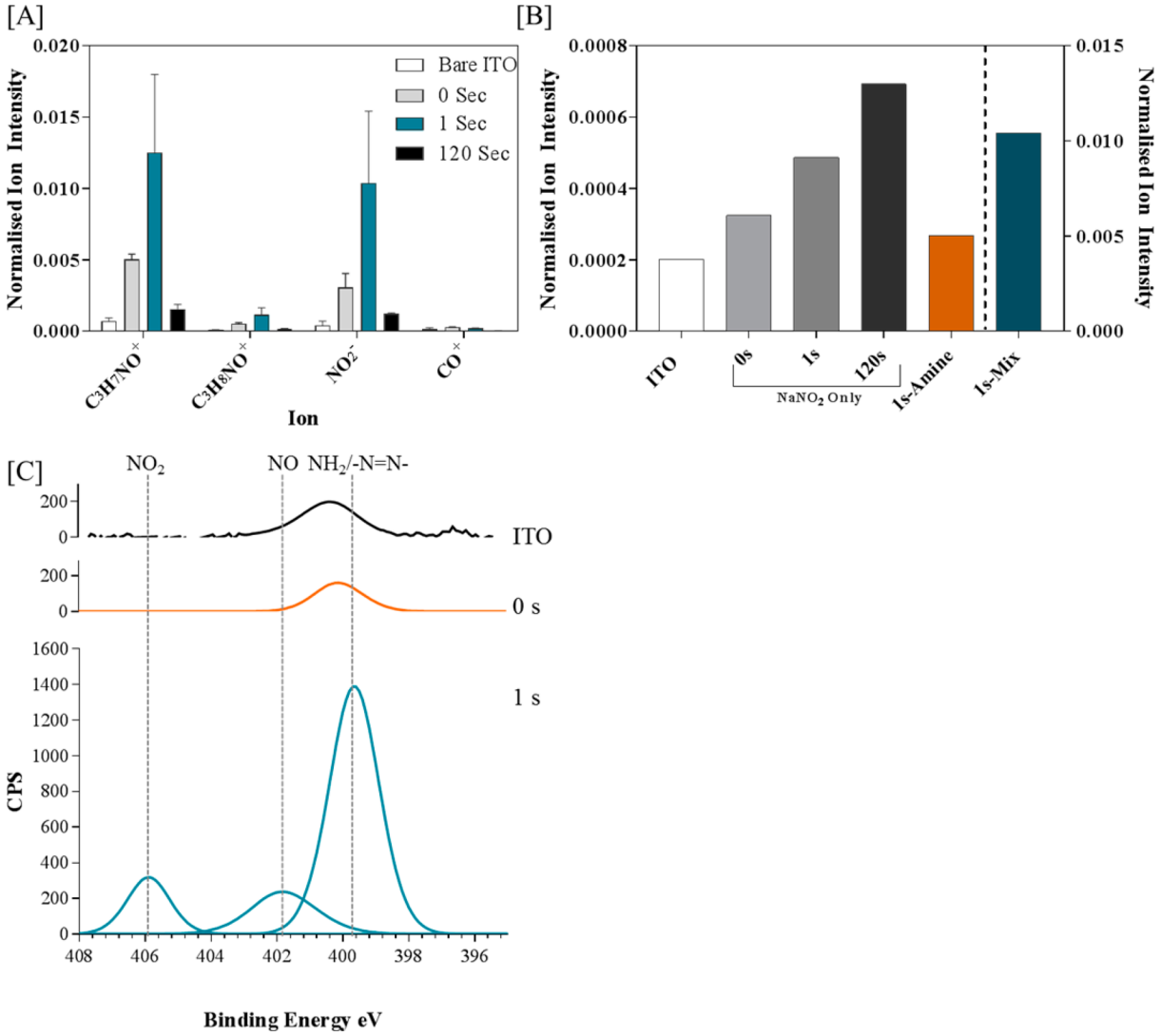

Figure 3. [A] Bar graph displaying normalized ion intensities for $C_3H_7NO^+$, $C_3H_8NO^+$, NO_2^-, and CO^+; error bars represent 1 standard deviation. Proposed chemical structures based on the chemical assignments are shown above the tallest bar for each ion. Two-way ANOVA was performed with Tukey post-test to test for significance against the bare ITO control. [B] NO_2^- ion peaks for ITO, 0 s, 1 s, and 120 s (all with $NaNO_2$ only), 1 s (*p*-phenylenediamine "amine" only), and 1 s complete mix (right *y*-axis). [C] XPS data displaying nitrogen peaks (N 1s, $n = 9$) for samples of bare ITO, 0 and 1 s grafted. Fitted peaks are displayed.

the region outside the grafted circle. For the thinner layers on the 1 and 2 s grafted surfaces there is a mixture of fragments including indium ions and fragments formed from the aryl layer; this is due to the aryl layer being thinner than the analysis depth of the ion beam which is approximately 4 nm.[38] Two methods were utilized to estimate the depth of the varying electrografted films: AFM depth profiling and ellipsometry (Table 2). Because of the limitations of ellipsometry, mainly that within our model the indices of refraction of the ITO and the aryl amine layer are very similar, for this reason the AFM depth profiling was necessary as an alternative method to measure the depth of the films. A summary of typical data obtained from the depth profiling can be seen in Figure S7.

From the data shown in Table 2, it can be seen that the layers range in thickness from approximately 2 to 26 nm. The standard deviations displayed in Table 2 are believed to arise from a combination of the limitations of the techniques and the heterogeneity of the surfaces. It is important to note that the surface roughness (R_a) of bare, clean ITO is approximately 0.8 nm with a standard deviation of ±0.03 nm. Considering that the standard deviation of the surface roughness at the 1 s grafted sample is ±1.1 nm indicates that the technique is sufficiently accurate to determine the film thickness even at the thinnest film. This data is in agreement with previous studies stating the maximum achieved diazonium-based aryl film formed on a surface by electrochemical reduction is

DOI: 10.1021/acs.langmuir.7b00494
Langmuir 2017, 33, 4924−4933

approximately 20 nm.[12,37] With a single aniline molecule being approximately 0.9 nm in diameter,[39] it would seem that even at the surface grafted for only 1 s aryl amine multilayers are exhibited at the surface of the electrode and become thicker with increased grafting time as indicated by the ellipsometry and AFM data. This is in agreement with the literature in which there are extensive descriptions and reports of multilayers formed with modification of surfaces by diazonium grafting.[34−36]

The nature of the bond formed from electrochemically grafting the *in situ* generated 4-aminobenzenediazonium to the ITO surface is yet to be established. Establishing the nature of the bond formed will be indicative of the mechanism. To elucidate the type of bond formed, we used ToF-SIMS to determine and compare the chemical fragments produced from four different samples which were an unmodified ITO; "0" s which was exposed to *in situ* generated 4-aminobenzenediazonium but without application of any applied potential to determine if any spontaneous electrografting occurs (see methods); 1 s electrografted and 120 s electrografted samples. When a fixed potential was applied for 1 s, it resulted in thinner aryl amine layers on the ITO than compared to longer electrografting times (Table 2). Therefore, electografted sample fragments formed by ToF-SIMS from the 1 s sample should contain ions formed from the ITO surface and the bond formed between the ITO and the first aryl layer. The results of this can be seen in Figure 3.

To determine the secondary ions that were likely to contain information relating to the bond to the ITO surface from the ToF-SIMS, the mass spectra peak list was initially filtered so only peaks that were exclusive in either the 1 or 0 s remained. The sample electrografted for 120 s was used as a negative control as the aryl amine layer will be so thick that fragments produced in ToF-SIMs will not contain ions from the surface of the ITO. A two-way ANOVA followed by a Sidak multiple comparison test was then conducted to isolate the peaks that were significantly different to the bare ITO control. Following this, two secondary ions in particular were isolated as being of interest to the binding of the aryl amine to the ITO surface: $C_3H_7NO^+$ ($p < 0.0001$) and $C_3H_8NO^+$ ($p = 0.01$). Considering the initial compound, these fragments can be arranged in two ways with the carbon binding to either the surface oxygen or the nitrogen. It is, however, the significantly increased $N{-}O^-$ ion in the 1 s and the lack of a $C{-}O^-$ ion that leads us to propose that the aryl amine is binding via a nitrogen and an oxygen and not via a carbon. Figure 3B further shows the presence of the NO_2^- ion peak in increasing intensity in samples that only came into contact with sodium nitrite. It is also interesting to note that with increased length of time the relative ion intensity associated with NO_2^- increases providing further evidence this is adsorbed on to the ITO surface, which is in contrast to that observed on copper.[40] We also performed CVs of $NaNO_2$ solutions (Figure S8) and an increase in charging current is seen when compared to the HCl control CV, but no faradaic events were observed. This presumably occurs due to ions associated with $NaNO_2$ adsorbing on the ITO supporting the ToF-SIMS data. This is also supported by the XPS data in Figure 3C, which displays the N 1s spectra for the ITO, 1 and 0 s samples. In the N 1s spectra, there are clear NH_2 peak at ∼400 eV and NO and NO_2 peaks at ∼402 and ∼406 eV, respectively.[41,42] There is a slight increase in the C−O peak[42] from the O 1s spectra in the XPS; however, as can be seen in the Supporting Information (Figure S1), there is high background carbon as well on the control sample (for wide-field spectra and O 1s see Supporting Information). After blank subtracting the ITO from the 1 s XPS data the C 1s and N 1s spectra data give a ratio of N:C of 1:6.78, which is what would be expected assuming we have complete reduction of the azo group to the aryl radical which then reacts with the surface yielding an amine functional group. Interestingly, the NO_2^- peaks observed are not found to the same magnitude when looking at the sodium nitrite samples only (Figure 3B). We tentatively infer from this that there is some sort of cooperative effect between the sodium nitrite and the *p*-phenylenediamine (Figure 4), although the exact details require further study.

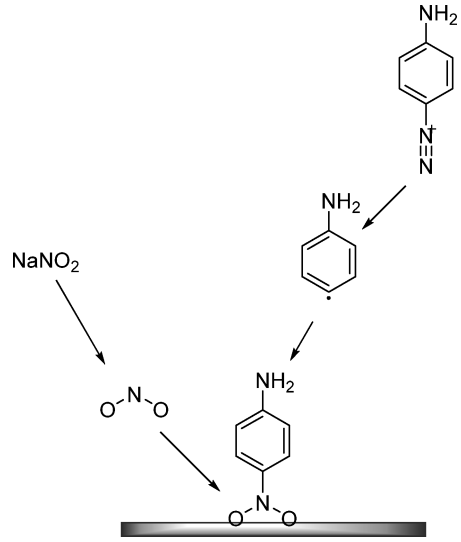

Figure 4. Schematic demonstrating aryl amine film formation on surface.

There also appears to be a small amount of spontaneous binding as can be seen by the presence of the $C_3H_7NO^+$ ion in the ToF-SIMS data for the "0" second grafted surface (Figure 3). There does not appear to be any spontaneous binding shown in the XPS data so if any spontaneous binding is occurring it is likely to be nominal compared to the reductive electrochemical binding.

Mechanisms proposed for diazonium binding shown on other surfaces such as gold and carbon (see Table 1) have indicated a carbon-based bond or a −N═N− bond. In our investigations we have identified an N−O bond, previously unseen for diazonium grafting, which suggests a different mechanism for diazonium binding at ITO to that previously observed at gold and carbon. Work by Hetemi et al.[33] has shown that while the diazonium is reduced to an aryl radical as expected, it is also possible to reduce sodium nitrate to nitrite which can then absorb to the surface. This support our assertions that sodium nitrite adsorb to ITO. As the diazonium cation is formed *in situ* from the reaction of sodium nitrite and *p*-phenylenediamine (in a 1:1 ratio), the data suggest that the NO_2 identified originates from unreacted sodium nitrite. This then provides a docking point for the aryl radical formed from the diazonium (as depicted in Figure 4). This is further supported by the presence of the same NO^- ion fragment when the diazonium grafting is conducted on gold (see Figure S2), further substantiating that an alternative reaction is occurring *in situ* than has been observed previously.

DOI: 10.1021/acs.langmuir.7b00494
Langmuir 2017, 33, 4924−4933

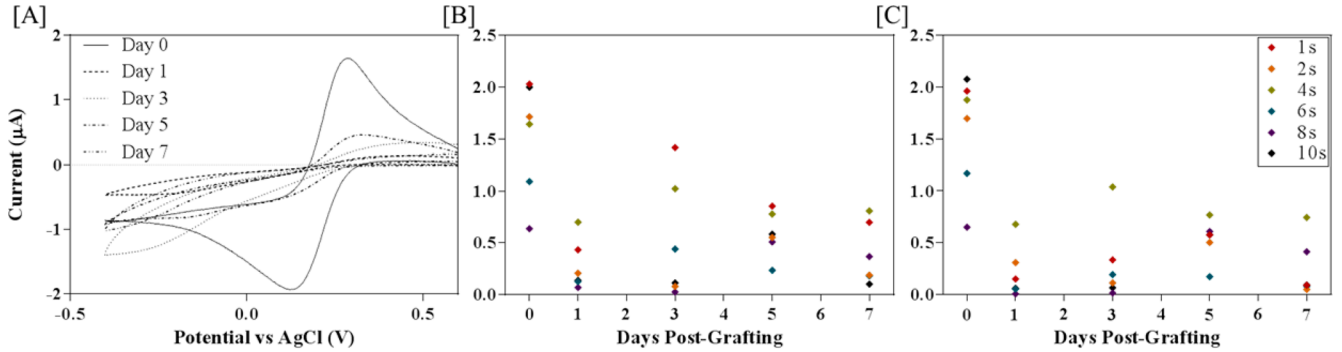

Figure 5. The *y*-axis label consistent for [A–C]. [A] CVs of 1 s grafted sample across 7 days in 250 μM potassium ferricyannide (PBS) at a scan rate of 100 mV/s between 0.6 and −0.4 V scanned initially in the negative direction. [B] Mean peak cathodic currents (I_{pc}) from all samples across 7 days with mean peak anodic currents (I_{pa}) shown in [C]; [B + C] *n* is between 4 and 8.

Stability of Aryl Amine Film. Stability of the aryl amine film will become an important factor if the ITO-SWCNT sensors are to ever be mass produced. Stability was studied electrochemically by performing cyclic voltammetry, across the different depth films, by using the well-characterized redox mediator ferricyanide ($[Fe(CN)_6]^{3-}$) as a standard redox probe, on day 0—the day that they were grafted—and days 3 and 7 postgrafting. The initial hypothesis for the films was that with time the oxidative and reductive peaks seen via CV run in the presence of ferricyanide would become larger as the film degrades and reveals the conductive nature of the ITO film beneath. However, as can be seen from Figure 5, the reverse of this is true.

It is apparent that from day 0 (Figure 5A) that the thinner aryl amine layers are not thick enough to passivate electron transfer to ferricyanide. Therefore, reductive and oxidative peaks can be seen at 0.130 and 0.286 V, respectively, as is shown for the 1 s grafted sample in Figure 5A. The peak currents also start at approximately 2 μA for both reductive (I_{pc}) and oxidative (I_{pa}) peak currents (Figure 5A, day 0), and the magnitudes of the peak currents decay with time, which can be seen in Figures 5B and 5C. This is seen consistently with all the film depths with an apparent inverse relationship between film thickness and peak current, as to be expected. We hypothesized from Figure 5 that the layer is not degrading which would reveal the ITO but rather material from the atmosphere is being adsorbed and passivating the surface with time. If films were not stable and the ITO surface was being revealed, cyclic voltammograms obtained in the presence of ferricyanide would result in a typical redox couple associated with ferricyanide as seen at day 0 (Figure 5A). On the contrary, this was not the case, and the peak current associated with the ferricyanide becomes smaller, which is indicative of a smaller electroactive area as governed by the Randles–Sevcik equation. It was therefore important to understand what is occurring at the surface to passivate the aryl amine layers. This was achieved by performing ToF-SIMS analysis on surfaces grafted and stored in air for several days (see Figures S3 and S4). We investigated the $C_6H_2^-$ peak, which was indicative of the diazonium-derived film's presence and establish that this was the case (Figure S4). A phenyl–NO peak was not chosen as this can only be detected in the thinnest layers as shown with the 1 s grafted sample due to narrow penetration of the ion beam.

Figure 6 shows that surfaces are prone to absorbing impurities from the atmosphere such as the characteristic

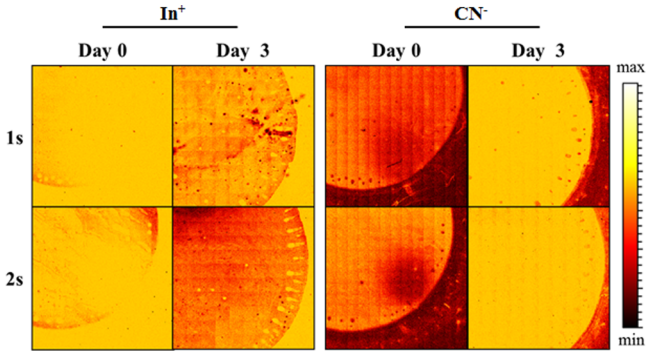

Figure 6. ToF-SIMS secondary ion images of In^{114+} in the figure legend (left) and CN^- (right) of samples grafted for either 1 or 2 s, scanned on day 0 and day 3. Scale bar indicative for all images.

CN^- shown in Figure 6. This can also be seen from the In^+ secondary ion images which show an increase in surface coverage with time as the In^+ ion intensity decreases. By combining the electrochemical data from the CVs (Figure 5) and the surface analysis from ToF-SIMS, it would appear that the aryl amine layers are stable throughout 7 days. As such, if they were to be mass produced, it would be necessary to store them either under an inert gas such as argon or under vacuum conditions prior to CNT coupling.

Calculation of Heterogeneous Rate Constant, k^0. Finally, samples of varying film thicknesses were used to construct various ITO–CNT sensor platforms, and the ability to tailor the electron transfer kinetics of the chips was investigated. To provide evidence that CNTs are physically bound to the ITO and the mechanism is not via adsorption, plain ITO and ITO functionalized with the aryl amine were exposed to CNTs, which had their carboxyl groups activated, via carbodiimide coupling chemistry, and characterized by SEM. SEM images were then taken (Figure S6). In the absence of the aryl amine tether layer very few CNTs were observed on the surface, suggesting a physical interaction between the CNTs and aryl amine is the mechanism of attachment. As the layers seem to passivate with time due to contaminants from the environment, in all cases CNTs were bound to the aryl layer immediately after grafting. Three different aryl thicknesses were utilized by grafting the aryl layer for either 1, 10, or 120 s. It was hypothesized that the thinner the aryl layer the faster and more efficient the electron transfer kinetics should be. Laforgue et al. showed that thin films on a surface exhibit no detectable barrier effect unlike thick films as seen in Figure 1.[18] They also showed

DOI: 10.1021/acs.langmuir.7b00494
Langmuir 2017, 33, 4924–4933

that the k^0_{App}, which is the apparent rate constant, is dependent not only on layer thickness but also on the homogeneity of the surface. Despite thinner layers being ideal, a monolayer, however, may not be. With a monolayer the conformational state is fixed, but when multilayers are present there is flexibility in the conformation which can give a higher conductivity.[43] As is clear from the ellipsometry and AFM scratching data (Table 2) even the layer grafted for 1 s is on average more than a monolayer in thickness, yet still very thin, which should result in more conductive and efficient final sensor when compared to the sensor made with the aryl layer grafted for 120 s.

The heterogeneous rate constant (k^0) was calculated for each CNT sensor using eq 1

$$\psi = k^0\left[\frac{\pi DnvF}{RT}\right]^{-0.5} \quad (1)$$

where ψ is a function of the peak separation as described by Nicholson and Shain,[44,45] D is the diffusion coefficient, n is the number of electrons transferred in the redox reaction, F is the Faraday constant, R is the gas constant, and T is the temperature. Whereas Nicholson and Shain's method for determining ψ is based on the assumption that the rate transfer coefficient, α, is 0.5, to get a more accurate value of ψ, α was calculated independently for each sensor. By plotting ψ versus $[\pi DnvF/RT]^{-0.5}$, k^0 can be determined from the slope of the resultant graph (Figure 6) (see Supporting Information for full calculations and graphs, Figure S5).

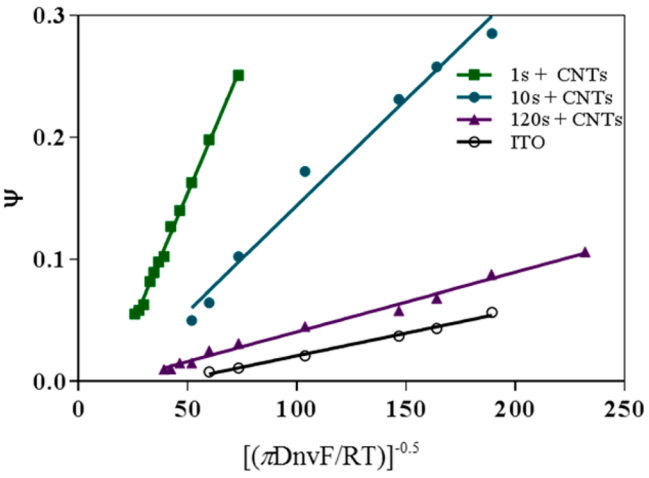

Figure 7. Nicholson plot to determine k^0 for ITO−CNT sensors constructed with aryl amine layers grafted for 1, 10, and 120 s. ITO only control is shown in black. N = 3. Scan rates plotted are between 20 mV/s and 1.6 V/s.

By decreasing the aryl amine film from ∼20 nm (120 s) to ∼2 nm (1 s) the k^0 is increased by an order of magnitude from 3.57×10^{-4} to 4.26×10^{-3} cm s^{-1} with the ∼5 nm aryl amine film (10 s) following the trend and having a k^0 of 1.74×10^{-3} cm s^{-1}. The ITO control also has a k^0 of only 3.7×10^{-4} cm s^{-1}, which is slower than all surfaces modified with CNTs. This gives direct evidence for the improvement in electron transfer rates of ITO−CNT sensors through the tailoring and thinning of the aryl amine film. One interpretation of the data is that the trend of increasing rate constant with thinner films results from greater access of the redox couple to the bare ITO as the aryl layer gets thinner. However, this can be discounted as we have previously reported that at the thickest film the electrochemistry (grafting time 120 s) associated with the ferricyanide is blocked.[2] Therefore, the fact that the rate constants are greater when aryl amine functionalized ITO is modified with CNTs in comparison to plain ITO, and we are observing electrochemistry associated with ferricyanide which is not observed at thicker films,[2] is evidence that it is the presence of the CNTs which results in the increased rate constants. Consequently, it is not due to increased access of the redox probe to the ITO as the films become thinner.

CONCLUSION

In this work we have shown evidence that the bond formed between an ITO substrate and a diazonium-based film to be N−O in nature, resulting from the reduction of diazonium and the physio-adsorption of excess sodium nitrite in solution. The depth of such films can be tailored by altering the length of time a current is passed through the substrate. The films are stable with time though prone to adsorb contaminates from the environment, as displayed by the increasing presence of the CN^- ion as a function of time in the ToF-SIMS data; therefore, binding of CNTs should ideally be done immediately to limit exposure to contaminants. Decreasing the aryl amine layer from ∼26 to ∼2 nm resulted in an increase in the heterogeneous rate constant, k^0, by an order of magnitude. Thus, we show the importance of molecularly controlling surface diazonium film thickness for improving the sensor kinetics.

ASSOCIATED CONTENT

Supporting Information

The Supporting Information is available free of charge on the ACS Publications website at DOI: 10.1021/acs.langmuir.7b00494.

Figures S1−S8 (PDF)

AUTHOR INFORMATION

Corresponding Author

*Phone 01157484698, e-mail frankie.rawson@nottingham.ac.uk (F.J.R.).

ORCID

Frankie J. Rawson: 0000-0002-4872-8928

Notes

The authors declare no competing financial interest.

ACKNOWLEDGMENTS

This work was supported by the Biotechnology and Biological Sciences Research Council and Leverhulme Trust (ECF/2013-603). Dr. F. J. Rawson would also like to thank the University of Nottingham for funding via his awarded Nottingham Research Fellowship.

ABBREVIATIONS

AFM, atomic force microscopy; CNTs, carbon nanotubes; DCC, dicyclohexylcarbodiimide; DMSO, dimethyl sulfoxide; ITO, indium tin oxide; SAMs, self-assembled monolayers; SWCNTs, single-walled carbon nanotubes; ToF-SIMS, time-of-flight secondary ion mass spectroscopy; XPS, X-ray photon spectroscopy.

DOI: 10.1021/acs.langmuir.7b00494
Langmuir 2017, 33, 4924−4933

REFERENCES

(1) Honeychurch, K. C. *Nanosensors for Chemical and Biological Applications: Sensing with Nanotubes, Nanowires and Nanoparticles*; Elsevier: 2014.

(2) Rawson, F. J.; Yeung, C. L.; Jackson, S. K.; Mendes, P. M. *Nano Lett.* **2013**, *13* (1), 1−8.

(3) Rawson, F. J.; Hicks, J.; Dodd, N.; Abate, W.; Garrett, D. J.; Yip, N.; Fejer, G.; Downard, A. J.; Baronian, K. H. R.; Jackson, S. K.; Mendes, P. M. Fast, Ultrasensitive Detection of Reactive Oxygen Species Using a Carbon Nanotube Based-Electrocatalytic Intracellular Sensor. *ACS Appl. Mater. Interfaces* **2015**, *7* (42), 23527−23537.

(4) Rawson, F. J.; Garrett, D. J.; Leech, D.; Downard, A. J.; Baronian, K. H. R. Electron transfer from Proteus vulgaris to a covalently assembled, single walled carbon nanotube electrode functionalised with osmium bipyridine complex: Application to a whole cell biosensor. *Biosens. Bioelectron.* **2011**, *26* (5), 2383−2389.

(5) Delamar, M.; Hitmi, R.; Pinson, J.; Saveant, J. M. Covalent modification of carbon surfaces by grafting of functionalized aryl radicals produced from electrochemical reduction of diazonium salts. *J. Am. Chem. Soc.* **1992**, *114* (14), 5883−5884.

(6) Allongue, P.; Delamar, M.; Desbat, B.; Fagebaume, O.; Hitmi, R.; Pinson, J.; Savéant, J.-M. Covalent Modification of Carbon Surfaces by Aryl Radicals Generated from the Electrochemical Reduction of Diazonium Salts. *J. Am. Chem. Soc.* **1997**, *119* (1), 201−207.

(7) Lyskawa, J.; Bélanger, D. Direct Modification of a Gold Electrode with Aminophenyl Groups by Electrochemical Reduction of in Situ Generated Aminophenyl Monodiazonium Cations. *Chem. Mater.* **2006**, *18* (20), 4755−4763.

(8) Paulik, M. G.; Brooksby, P. A.; Abell, A. D.; Downard, A. J. Grafting Aryl Diazonium Cations to Polycrystalline Gold: Insights into Film Structure Using Gold Oxide Reduction, Redox Probe Electrochemistry, and Contact Angle Behavior. *J. Phys. Chem. C* **2007**, *111* (21), 7808−7815.

(9) Menanteau, T.; Levillain, E.; Downard, A. J.; Breton, T. Evidence of monolayer formation via diazonium grafting with a radical scavenger: electrochemical, AFM and XPS monitoring. *Phys. Chem. Chem. Phys.* **2015**, *17* (19), 13137−13142.

(10) Lamberti, F.; Agnoli, S.; Brigo, L.; Granozzi, G.; Giomo, M.; Elvassore, N. Surface Functionalization of Fluorine-Doped Tin Oxide Samples through Electrochemical Grafting. *ACS Appl. Mater. Interfaces* **2013**, *5* (24), 12887−12894.

(11) Chen, X.; Chockalingam, M.; Liu, G.; Luais, E.; Gui, A. L.; Gooding, J. J. A Molecule with Dual Functionality 4-Aminophenylmethylphosphonic Acid: A Comparison Between Layers Formed on Indium Tin Oxide by In Situ Generation of an Aryl Diazonium Salt or by Self-Assembly of the Phosphonic Acid. *Electroanalysis* **2011**, *23* (11), 2633−2642.

(12) Mévellec, V.; Roussel, S.; Tessier, L.; Chancolon, J.; Mayne-L'Hermite, M.; Deniau, G.; Viel, P.; Palacin, S. Grafting Polymers on Surfaces: A New Powerful and Versatile Diazonium Salt-Based One-Step Process in Aqueous Media. *Chem. Mater.* **2007**, *19* (25), 6323−6330.

(13) Picot, M.; Lapinsonnière, L.; Rothballer, M.; Barrière, F. Graphite anode surface modification with controlled reduction of specific aryl diazonium salts for improved microbial fuel cells power output. *Biosens. Bioelectron.* **2011**, *28* (1), 181−188.

(14) Pinson, J.; Podvorica, F. Attachment of organic layers to conductive or semiconductive surfaces by reduction of diazonium salts. *Chem. Soc. Rev.* **2005**, *34* (5), 429−39.

(15) Stewart, M. P.; Maya, F.; Kosynkin, D. V.; Dirk, S. M.; Stapleton, J. J.; McGuiness, C. L.; Allara, D. L.; Tour, J. M. Direct Covalent Grafting of Conjugated Molecules onto Si, GaAs, and Pd Surfaces from Aryldiazonium Salts. *J. Am. Chem. Soc.* **2004**, *126* (1), 370−378.

(16) de Villeneuve, C. H.; Pinson, J.; Bernard, M. C.; Allongue, P. Electrochemical Formation of Close-Packed Phenyl Layers on Si(111). *J. Phys. Chem. B* **1997**, *101* (14), 2415−2420.

(17) D'Amour, M.; Bélanger, D. Stability of Substituted Phenyl Groups Electrochemically Grafted at Carbon Electrode Surface. *J. Phys. Chem. B* **2003**, *107* (20), 4811−4817.

(18) Laforgue, A.; Addou, T.; Bélanger, D. Characterization of the Deposition of Organic Molecules at the Surface of Gold by the Electrochemical Reduction of Aryldiazonium Cations. *Langmuir* **2005**, *21* (15), 6855−6865.

(19) Mesnage, A.; Lefèvre, X.; Jégou, P.; Deniau, G.; Palacin, S. Spontaneous Grafting of Diazonium Salts: Chemical Mechanism on Metallic Surfaces. *Langmuir* **2012**, *28* (32), 11767−11778.

(20) Kesavan, S.; Abraham John, S. Spontaneous grafting: A novel approach to graft diazonium cations on gold nanoparticles in aqueous medium and their self-assembly on electrodes. *J. Colloid Interface Sci.* **2014**, *428*, 84−94.

(21) Small, L. J.; Hibbs, M. R.; Wheeler, D. R. Spontaneous Aryldiazonium Film Formation on 440C Stainless Steel in Non-aqueous Environments. *Langmuir* **2014**, *30* (47), 14212−14218.

(22) Civit, L.; Fragoso, A.; O'Sullivan, C. K. Thermal stability of diazonium derived and thiol-derived layers on gold for application in genosensors. *Electrochem. Commun.* **2010**, *12* (8), 1045−1048.

(23) Shewchuk, D. M.; McDermott, M. T. Comparison of diazonium salt derived and thiol derived nitrobenzene layers on gold. *Langmuir* **2009**, *25* (8), 4556−63.

(24) Liu, G.; Böcking, T.; Gooding, J. J. Diazonium salts: Stable monolayers on gold electrodes for sensing applications. *J. Electroanal. Chem.* **2007**, *600* (2), 335−344.

(25) Mirri, F.; Ma, A. W. K.; Hsu, T. T.; Behabtu, N.; Eichmann, S. L.; Young, C. C.; Tsentalovich, D. E.; Pasquali, M. High-Performance Carbon Nanotube Transparent Conductive Films by Scalable Dip Coating. *ACS Nano* **2012**, *6* (11), 9737−9744.

(26) Snow, E. S.; Novak, J. P.; Campbell, P. M.; Park, D. Random networks of carbon nanotubes as an electronic material. *Appl. Phys. Lett.* **2003**, *82* (13), 2145−2147.

(27) Kaempgen, M.; Duesberg, G. S.; Roth, S. Transparent carbon nanotube coatings. *Appl. Surf. Sci.* **2005**, *252* (2), 425−429.

(28) Small, W. R.; Walton, C. D.; Loos, J. in het Panhuis, M. Carbon Nanotube Network Formation from Evaporating Sessile Drops. *J. Phys. Chem. B* **2006**, *110* (26), 13029−13036.

(29) Rao, S. G.; Huang, L.; Setyawan, W.; Hong, S. Nanotube electronics: Large-scale assembly of carbon nanotubes. *Nature* **2003**, *425* (6953), 36−37.

(30) Garrett, D. J.; Flavel, B. S.; Shapter, J. G.; Baronian, K. H. R.; Downard, A. J. Robust Forests of Vertically Aligned Carbon Nanotubes Chemically Assembled on Carbon Substrates. *Langmuir* **2010**, *26* (3), 1848−1854.

(31) Menanteau, T.; Levillain, E.; Breton, T. Spontaneous Grafting of Nitrophenyl Groups on Carbon: Effect of Radical Scavenger on Organic Layer Formation. *Langmuir* **2014**, *30* (26), 7913−7918.

(32) Adenier, A.; Bernard, M.-C.; Chehimi, M. M.; Cabet-Deliry, E.; Desbat, B.; Fagebaume, O.; Pinson, J.; Podvorica, F. Covalent Modification of Iron Surfaces by Electrochemical Reduction of Aryldiazonium Salts. *J. Am. Chem. Soc.* **2001**, *123* (19), 4541−4549.

(33) Hetemi, D.; Combellas, C.; Kanoufi, F.; Pinson, J.; Podvorica, F. I. Surface modification by electrochemical reduction of alkyldiazonium salts. *Electrochem. Commun.* **2016**, *68*, 5−9.

(34) Bernard, M.-C.; Chaussé, A.; Cabet-Deliry, E.; Chehimi, M. M.; Pinson, J.; Podvorica, F.; Vautrin-Ul, C. Organic Layers Bonded to Industrial. *Chem. Mater.* **2003**, *15* (18), 3450−3462.

(35) Kariuki, J. K.; McDermott, M. T. Nucleation and Growth of Functionalized Aryl Films on Graphite Electrodes. *Langmuir* **1999**, *15* (19), 6534−6540.

(36) Greenwood, J.; Phan, T. H.; Fujita, Y.; Li, Z.; Ivasenko, O.; Vanderlinden, W.; Van Gorp, H.; Frederickx, W.; Lu, G.; Tahara, K.; Tobe, Y.; Uji-i, H.; Mertens, S. F. L.; De Feyter, S. Covalent Modification of Graphene and Graphite Using Diazonium Chemistry: Tunable Grafting and Nanomanipulation. *ACS Nano* **2015**, *9* (5), 5520−5535.

DOI: 10.1021/acs.langmuir.7b00494
Langmuir 2017, 33, 4924−4933

(37) Pinson, J. Attachment of Organic Layers to Materials Surfaces by Reduction of Diazonium Salts. *In Aryl Diazonium Salts*; Wiley-VCH Verlag GmbH & Co. KGaA: 2012; pp 1−35.
(38) Group, E. A. Time-of-Flight Secondary Ion Mass Spectrometry, TOF-SIMS Analysis; http://www.eag.com/mc/time-of-flight-secondary-ion-mass-spectrometry.html (accessed 22.06.16).
(39) Yang, L. Y. O.; Chang, C.; Liu, S.; Wu, C.; Yau, S. L. Direct Visualization of an Aniline Admolecule and Its Electropolymerization on Au(111) with in Situ Scanning Tunneling Microscope. *J. Am. Chem. Soc.* **2007**, *129* (26), 8076−8077.
(40) Shul, G.; Parent, R.; Mosqueda, H. A.; Bélanger, D. Localized In situ Generation of Diazonium Cations by Electrocatalytic Formation of a Diazotization Reagent. *ACS Appl. Mater. Interfaces* **2013**, *5* (4), 1468−1473.
(41) Mendes, P.; Belloni, M.; Ashworth, M.; Hardy, C.; Nikitin, K.; Fitzmaurice, D.; Critchley, K.; Evans, S.; Preece, J. *ChemPhysChem* **2003**, *4* (8), 884−889.
(42) Moulder, J. F.; Chastain, J. *Handbook of X-ray Photoelectron Spectroscopy: A Reference Book of Standard Spectra for Identification and Interpretation of XPS Data*; Physical Electronics Division, Perkin-Elmer Corporation: 1992.
(43) McCreery, R.; Dieringer, J.; Solak, A. O.; Snyder, B.; Nowak, A. M.; McGovern, W. R.; DuVall, S. Molecular Rectification and Conductance Switching in Carbon-Based Molecular Junctions by Structural Rearrangement Accompanying Electron Injection. *J. Am. Chem. Soc.* **2003**, *125* (35), 10748−10758.
(44) Nicholson, R. S.; Shain, I. Theory of Stationary Electrode Polarography. Single Scan and Cyclic Methods Applied to Reversible, Irreversible, and Kinetic Systems. *Anal. Chem.* **1964**, *36* (4), 706−723.
(45) Lavagnini, I.; Antiochia, R.; Magno, F. An Extended Method for the Practical Evaluation of the Standard Rate Constant from Cyclic Voltammetric Data. *Electroanalysis* **2004**, *16* (6), 505−506.

DOI: 10.1021/acs.langmuir.7b00494
Langmuir 2017, 33, 4924−4933